Journal of Applied Fluid Mechanics, Vol. 10, No. 3, pp. 925-932, 2017.
Available online at www.jafmonline.net, ISSN 1735-3572, EISSN 1735-3645.
DOI: 10.18869/acadpub.jafm.73.240.27033

Determining the Thin Film Thickness of Two Phase Flow using Optics and Image Processing

G. C. Keerthi Vasan and M. Venkatesan†

SASTRA University, Thanjavur, India

†*Corresponding Author Email: mvenkat@mech.sastra.edu*

(Received August 6, 2016; accepted February, 5, 2017)

ABSTRACT

Gas- Liquid flows are by far the most important type of multiphase flow. This can be attributed to the wide range of industrial applications that the gas-liquid flow is discerned in. Popular examples of Gas-liquid flows are oil-gas mixtures, evaporators, boilers, condensers, refrigeration and cryogenics. The measurement of the liquid film thickness in two phase flows is prominent in various heat and mass transfer applications such as in boilers. To determine the thin film thickness is the aim of this study. A glass tube of diameter 4.7 mm is used for conducting the experiment and a laser pointer is used to obtain an image pattern on the screen. Using the principles of Optics, a method has been proposed to determine the thin film thickness and also to characterize the different types of flow. The thin film thickness obtained in the proposed method is validated using Image Processing.

Keywords: Two phase flow; Thin film thickness; Optics; Image processing.

1. INTRODUCTION

Two phase flow is the simultaneous flow of two different substances or the same substance in two different phases. It is only a particular example of multiphase flow. Their study has gained much importance in recent times due to their increasing applications.

One of the earliest seminal research on determining the thin-film thickness was conducted by Dallman (1978) using a very thin conductive probe. The study of two phase flow patterns were carried out by Coleman and Garimella (1999) by using High Speed Videography techniques. In the two phase flow of fluids, if the capacitance of the two substances taken are distinct, then the capacitance value obtained can be used to determine the liquid film thickness. This capacitive measurement of the film thickness was done by Chen *et al*. (1996). Measurement of liquid film thickness in air-water two phase flows was carried out by Seshadri *et al*. (2015) using Image Processing. The photographs of the flow regimes that were captured using a high speed camera were later processed and optimized using Image processing techniques to obtain the thin film thickness.

The study of two phase flows has slowly drifted towards the fields of Optics and Photonics considering their pronounced advancements. Shedd and Newell (1998) determined the thin film thickness by capturing the reflection of light from a liquid film using a charge coupled device camera. Barrau *et al*. (1999) by using optical probes placed in the flow were able to determine the void fraction and gas velocities locally. Mouza *et al*. (2000) used laser absorption methods to measure the liquid film thickness. The method is based on the absorption of light when passed through a dyed liquid and makes use of small laser sources and light sensors to accurately determine the thin film thickness. Farias *et al*. (2012) characterized the liquid film in liquid-gas flows using time-resolved LASER-induced fluorescence. Liquid slug and pig flow pattern determination in a horizontal gas liquid pipe was studied by Ruixi *et al*. (2013) by using an infrared ray and laser. Jagannathan *et al*. (2015) characterised the gas-liquid two phase flow patterns based on Laser Patterns. The prominent variation in the laser patterns obtained during the start and end of a bubble was used for the characterization. Xue *et al*. (2015) focused on the measurement of thickness in two phase gas-liquid annular flow using LIF (Laser Induced Fluorescence) technique. High speed photography is also incorporated to facilitate the measurement of the thin film thickness and also the flow evolution.

Balasubramanian *et al*. (1972) explored the feasibility of using Holographic interferometry to monitor the thin film thickness. This has led to a lot of research works based on Holographic and confocal microscopic principles. Lai *et al*. (2011) characterized the thin film thickness in thin film

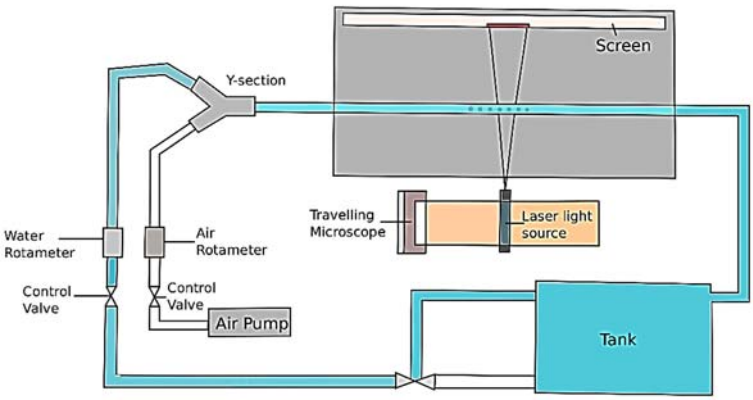

Fig. 1. Schematics of the experimental setup for air-water two phase flow The actual experimental setup is provided below for reference.

materials by the development of a digital holographic microscope. Various methods for thin film thickness measurement has been done through numerical analysis as well. Lakehal (2011) has given a thorough review on the use of CMFD code for the analysis of real coupled two-phase heat transfer problems. Level set approach is used by the code to solve the problem. To solve 3D problems, an automatized version of the code is employed which uses IST (Immersed Surfaces Technique) to transform the problem into a simple Cartesian grid.

It is evident from the above literature that there are very few methods in existence that are used to find the thin film thickness in two phase flows. And most of the available methods involve the use of high speed photography. Since two phase flows are of great industrial and scientific significance, there arises a need to devise a technique that is simple in finding the thin film thickness without compromising for accuracy in measurement. This study uses the principles of Optics to devise a method for finding out the thin film thickness in Air-Water two phase flows in a glass tube of diameter 4.7 mm. The results obtained using this method are validated using Image Processing.

2. IMAGE PROCESSING PROCEDURES

2.1 Inverting the Image

Image inversion is a technique in which the light areas are mapped progressively to dark ones and the dark areas are mapped to Light ones. The characterisation of pixel color gradients becomes substantially easier by Inversion of the Image.

2.2 Finding the Pixel Intensity

Byte image is one of the most common pixel format available and the number is stored as an 8 bit integer. The range of possible values for the pixels are from 0 to 255. (0, 0, 0) represents a complete black pixel and (255,255,255) a white pixel. The pixel format is (red, green, blue) and to represent coloured images, a vector sum of the three numbers is obtained and the resultant value is used to represent the image.

By rastering the entire image using an iterative loop, the pixel intensity per column is found.

2.3 Finding the Pixel Height

The determination of pixel height of the pattern is done in two ways: The manual way of finding the pixel height is by using the measure tool in GIMP (an open-source image editing software package) and placing the cursor between two desired points of interest. The pixel height is calculated inherently by the software package.

By using the Python Image Library (PIL), the bounds for the pixels are specified and an iterative loop is run in order to determine the pixel height. This is a more reliable and accurate method, but is time consuming and the computational time increases with the increase in size of the image. But it is this method that the present study utilizes for finding the pixel height.

3. EXPERIMENTAL SETUP

The schematics of the experimental setup is presented in Fig. 1. The experiment is carried out on a Borosilicate Glass of 4.7 mm diameter. Air and water are supplied by separate pumps and the volumetric flow rate is determined using respective rotameters. The experiment is carried out at the Heat transfer laboratory, School of Mechanical Engineering, SASTRA university.

Normal tap water with TDS (Total Dissolved Solids) concentration of 430 ppm is pumped using a 1400 Lph, 27 W water pump from an open tank. Air is blown at slightly above atmospheric pressure by a 240-Lph 3-W diaphragm-type air pump. Air and water are mixed in a Y-section. The mixture is passed to the glass tube. By varying the different flow parameters, different regimes of flow such as slug, slug train, bubble and bubble trains is obtained.

The Laser source is a 650 nm laser pointer which is

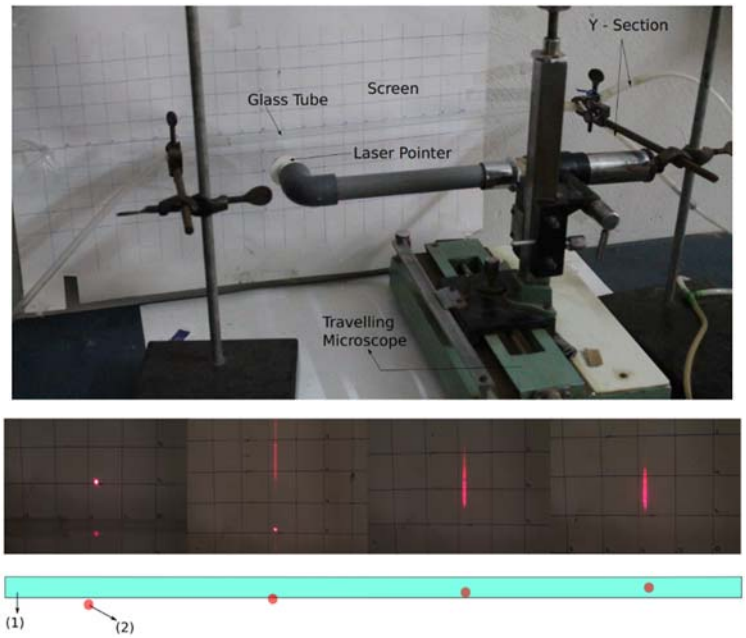

Fig. 2. Various Possibilities of placing the laser pointer (1). Glass Tube with single phase flow of water (2).Position of Laser pointer during the capture of image. From Left to Right-eccentricity (e) from center - (-3) mm, (-2.8) mm, (-1.5) mm, 0 mm.

fixed on a travelling microscope for obtaining precise and accurate positioning. The superficial velocities of gas and liquid are in the range of (0.3 to 1.5) m/s and (0.2 to 0.4) m/s respectively. The length of the tube is 30 cm and the temperature of the water is maintained in the range of 29 − 30o C.

In the present study, the distance between the laser source and the screen is maintained at 15 cm, the distance between the center of the glass tube and the screen at 7 cm. The Laser patterns are captured with a Canon EOS 1100D DSLR camera, which is later transferred to GIMP for processing.

3.1 Placement of the Laser Pointer

All possible positions for the placement of the laser pointer is carried out in order to determine the optimal position for determining the thin film thickness. These possibilities are illustrated in Fig. 2. From the possibilities obtained, it is concluded that the best choice for placing the laser pointer is eccentric from the center. And in this current study the eccentricity (e) has been chosen as (-1.5) mm (minus sign indicating below the center and positive sign above the center of the glass tube) The importance of eccentricity in the study is discussed in Results and Discussion.

3.2 Single Phase Study

A single phase flow study is carried out to study the characteristic laser patterns produced when there is only air or water flowing in the tube. These serve as base patterns to compare the image patterns produced during two phase flows.

A discussion of the importance of this study is presented in Results and Discussion.

4. RESULTS AND DISCUSSION

4.1 Determination of Flow Regimes

The determination of flow regimes is achieved by processing the image using the PIL (python image library). The total number of red pixels in Image are calculated by iterating through every pixel in the image. The plot of the Total number of red pixels in Image v/s the image column index along with a pictorial representation of the peaks is shown in Fig. 3.

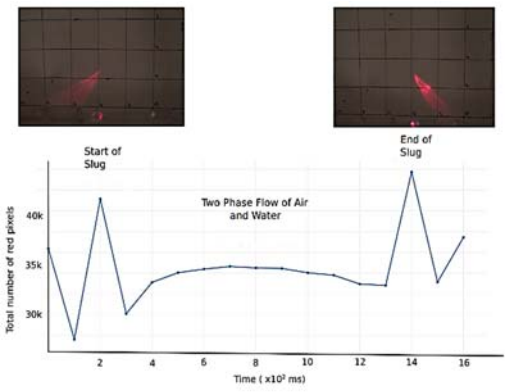

Fig. 3. Plot of Time (x 102 ms) v/s Total number of Red pixels in Image for a Slug.

There are two peaks, one during the start and the other at the end that are a characteristic of the refraction of light off the curvature of the bubble. By finding the time difference between the occurrence of the initial and terminal peaks, the type of flow is decided.

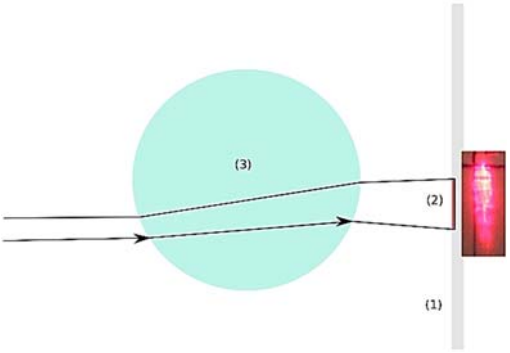

Fig. 4. Interaction of Laser Light impinging eccentric at the Glass Tube with single phase flow of air (1).Screen (2).Image Pattern Obtained (3).Air.

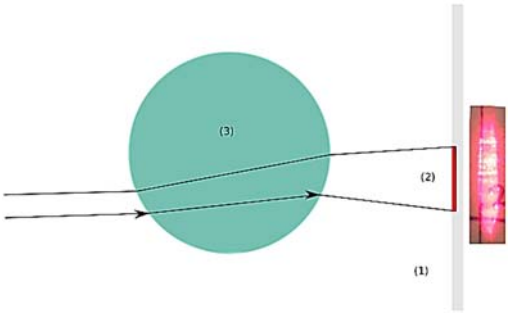

Fig. 5. Interaction of Laser Light impinging eccentric at the Glass Tube with single phase flow of water (1).Screen (2).Image Pattern Obtained (3).Water.

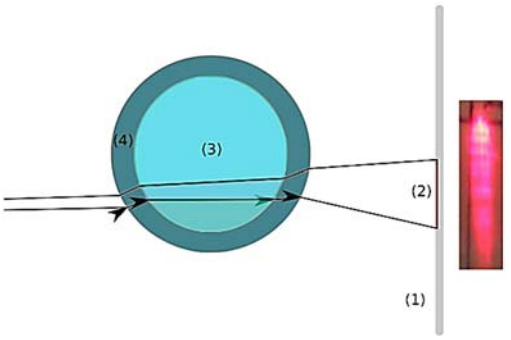

Fig. 6. Interaction of Laser Light impinging eccentric at the Glass Tube with two phase flow of water and air (1).Screen (2).Image Pattern Obtained (3).Air (4).Water.

Bubbles have little or no time difference between the initial and terminal peaks, whereas slugs have a larger time difference. By measuring the time difference, superficial liquid and gas velocities of medium and the frame rate of the camera, the length of the slug is determined.

4.2 Determining the Thin Film Thickness

In order to measure the thin film thickness, the extension of the image pattern when the laser light impinges on a glass tube during two phase flow is used for analysis. (see Fig. 6)

4.2.1 A study of the Image Extension During

Two phase flow According to Snell's law: (See Figs. 4, 5, 6 for reference)

$$n_1 Sin(\theta_1) = n_2 Sin(\theta_2) \quad (1)$$

where θ1 and θ2 are the angles of incidence and refraction for the upper light ray, and n1 and n2 are the refractive indices of mediums 1 and 2.

$$n_1 Sin(\alpha_1) = n_2 Sin(\alpha_2) \quad (2)$$

where α1 and α2 are the angles of incidence and refraction for the lower light ray.

Since, it is known that the α1 > θ1, it follows that α2 > θ2. Hence the extended image pattern obtained.

As a result of the Snell's law, the eccentricity of the laser affects the length of the image pattern obtained. An eccentricity of 1.5 mm below the center of the glass tube is chosen for this study as this offers the most prominent extended image pattern.

4.2.2 Modeling the Thin Film Thickness

To model the thin film thickness, without the loss of generality only the collective interaction of the entire setup is considered i.e due to the presence of a thin film, there is a lateral shift and we model only this by using the principles of Optics. The other interactions that might occur in the glass during the intermittent stages are ignored as they do not contribute to the image pattern obtained on the screen. The model is illustrated in Fig.7.

From the virtue of trigonometry,

$$t = y * \sin(k) \quad (3)$$

And the value for the angle k is found out from,

$$\tan(k) = \frac{d}{y} \quad (4)$$

The thin film thickness t is given by:

$$t = \frac{y * d}{\sqrt{d^2 + y^2}} \quad (5)$$

But since the thin film thickness is present on both the side of the glass tube, the quantity must be divided by a factor of 2. Therefore:

$$t = \frac{y * d}{2 * \sqrt{d^2 + y^2}} \quad (6)$$

4.2.3 Determining the Tube Thickness Using the Above Model

For a single phase flow of air in the tube, the model is employed. This enabled the determination of the Tube Thickness without any physical measurement. The tube thickness is found out to be 0.2 mm and this value matches the value obtained through measurement as well. Although determined, the study proceeds ignoring its effects, for the sake of simplicity.

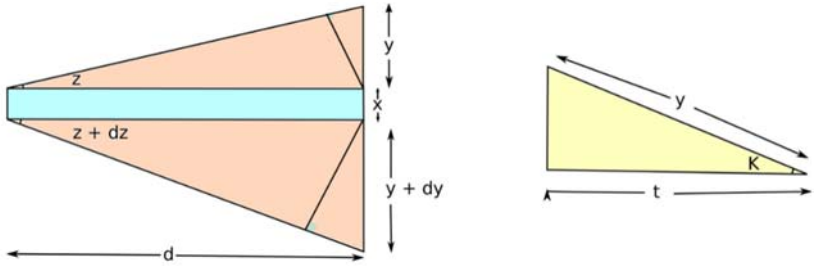

Fig. 7. Modelling the Thin Film Thickness Here (i) x is the diametrical length of the laser source (i.e the diameter of the image pattern on the screen without the glass tube), (ii) d is the distance between the laser source and the screen, and (iii) y,y+dy denotes the deviation of the image pattern from 'x' due to the presence of a thin film.

Table 1 Comparison of the thin film thickness obtained using Optical and Image Processing techniques for slug and slug trains

S No	Type of Flow	Superficial Liquid Velocity (m/s)	Superficial Gas Velocity (m/s)	Thin Film thickness using optical technique(t1) (± 0.01 mm)	Thin Film thickness using image processing(t2) (± 0.005 mm)	Error (t1-t2) (± 0.015 mm)
1	Slug and Slug Trains	0.3	0.4	0.62	0.49	0.13
		0.4	0.4	0.60	0.46	0.14
		0.5	0.4	0.59	0.45	0.14
		0.6	0.4	0.56	0.44	0.12
		0.7	0.4	0.54	0.42	0.12
		0.8	0.4	0.52	0.40	0.12
		0.3	0.4	0.71	0.52	0.19
		0.4	0.3	0.66	0.49	0.17
		0.5	0.3	0.64	0.48	0.16
		0.6	0.3	0.60	0.46	0.14
		0.7	0.3	0.58	0.45	0.13
		0.8	0.3	0.57	0.41	0.16
		0.3	0.2	0.72	0.57	0.15
		0.4	0.2	0.65	0.55	0.10
		0.5	0.2	0.64	0.53	0.11
		0.6	0.2	0.62	0.52	0.10
		0.7	0.2	0.60	0.49	0.11

4.2.4 Thin-Film Thickness

From the above model, by determining the divergence of the laser pattern (y) and fixing the distance between the laser source and the screen, the thin film thickness 't' is determined.

In this current study, distance between source and screen was fixed at 15 cm and consequently, the results follow for a superficial liquid velocity of (0.3 -1.5) m/s and superficial gaseous velocity of (0.2-0.4) m/s respectively is presented in Tables 1 and 2.

5. VALIDATION USING IMAGE PROCESS-ING.

High speed photographs of the top view of the flow are captured using a DSLR camera. The same flow parameters used for the previous study is used for the validation as well.

5.1 The Need for Dyes

To determine the thin film thickness using image processing, initial experiments were conducted on tap water. But this posed a huge challenge. It was extremely hard to distinguish between the water and the glass as they have similar refractive indices. Even after subsequent Image Processing, it was still hazy whether it was a reflection of the glass or the thin film itself that was recorded.

As a result of which, dyes were chosen for the analysis. Thick Blue dye is mixed up with the incoming water flow. This boosted the blue pixel intensities and thereby enhanced the display of the thin film thickness during image processing. It was this method that proved more reliable than the previous technique due to the clear distinction between the glass and the thin film during processing. A comparison is provided in the Fig. 8 and 9.

It is found out that the introduction of the dye did not affect the nature of flow patterns obtained during experimentation. The flow patterns with and without the introduction of a dye remained the same.

5.2 Image Processing Technique

Using the PIL (Python Image Library), every row is

Table 2 Comparison of the thin film thickness obtained using Optical and Image Processing techniques for Bubble and Bubble trains

S No	Type of Flow	Superficial Liquid Velocity (m/s)	Superficial Gas Velocity (m/s)	Thin Film thickness using optical technique(t1) (± 0.01 mm)	Thin Film thickness using image processing(t2) (± 0.005 mm)	Error (t1-t2) (± 0.015 mm)
2	Slug and Slug Trains	1	0.4	0.84	0.77	0.07
		1.1	0.4	0.83	0.73	0.10
		1.2	0.4	0.81	0.70	0.11
		1.3	0.4	0.80	0.68	0.12
		1.4	0.4	0.74	0.66	0.08
		1.5	0.4	0.70	0.65	0.05
		1.0	0.3	0.91	0.85	0.06
		1.1	0.3	0.85	0.83	0.02
		1.2	0.3	0.81	0.81	0.00
		1.3	0.3	0.79	0.77	0.02
		1.4	0.3	0.76	0.74	0.02
		1.5	0.3	0.72	0.69	0.03
		1.1	0.2	1.3	1.25	0.05
		1.2	0.2	1.22	1.18	0.04
		1.3	0.2	1.1	1.07	0.04
		1.4	0.2	0.98	0.92	0.06
		1.5	0.2	0.9	0.86	0.04

rastered and the cumulative pixel intensity of each row is plotted. This procedure is carried out with single phase flows of water and air. From the single phase flows, extremal baselines are established. The pixel intensity of two phase flow as a result, lies bounded between the two extremal regions. By measuring the deviation of the pixel intensities, the pixel intensity of the thin film thickness is determined. And the obtained pixel intensities is modelled to determine the thin film thickness.

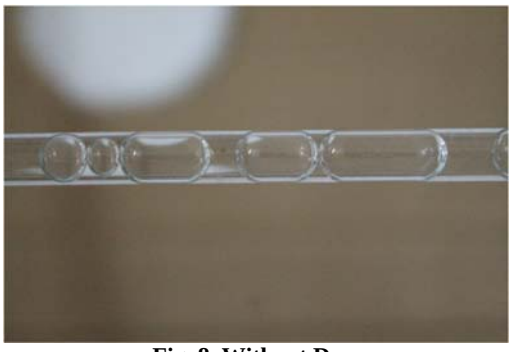

Fig. 8. Without Dye.

The plot of the Image Column Index v/s the Pixel Intensity is shown in Fig.10 .The wide range of values (but bounded) for the flows are due to the fact that the images were taken at various times of the day. And the amount of sunlight present at the time of experimentation affected the range of Pixel Intensities.

5.3 Modelling the Thin Film Thickness

Let G be the thin film thickness and it is a function of the pixel height (P) and the type of flow regime (R) : G = (f (P,R)).

R	Type of Flow
-1	Single phase flow of air
0	Two phase flow of air and water
1	Single phase flow of water

Fig. 9. With Dye.

A linear regression of the following characteristic equation is assumed.

$$G = (a_1 P + a_2 R + a_3) \tag{7}$$

Using the Least squares regression analysis, the coefficient of the characteristic equation are found out. The coefficients are time variant and as a result of which velocity variant, and vary for every slug/ bubble train. It is assumed that the velocity variation in the passage of one slug train is infinitesimal and thereby enabling the use of a regression.

$$\sum_{i=1}^{\infty} \begin{bmatrix} P_i^2 & P_i R_i & R_i \\ P_i R_i & R_i^2 & P_i \\ R_i & P_i R_i & 1 \end{bmatrix} \begin{bmatrix} a_1 \\ a_2 \\ a_3 \end{bmatrix} = \sum_{i=1}^{\infty} \begin{bmatrix} P_i G_i \\ R_i G_i \\ G_i \end{bmatrix} \tag{8}$$

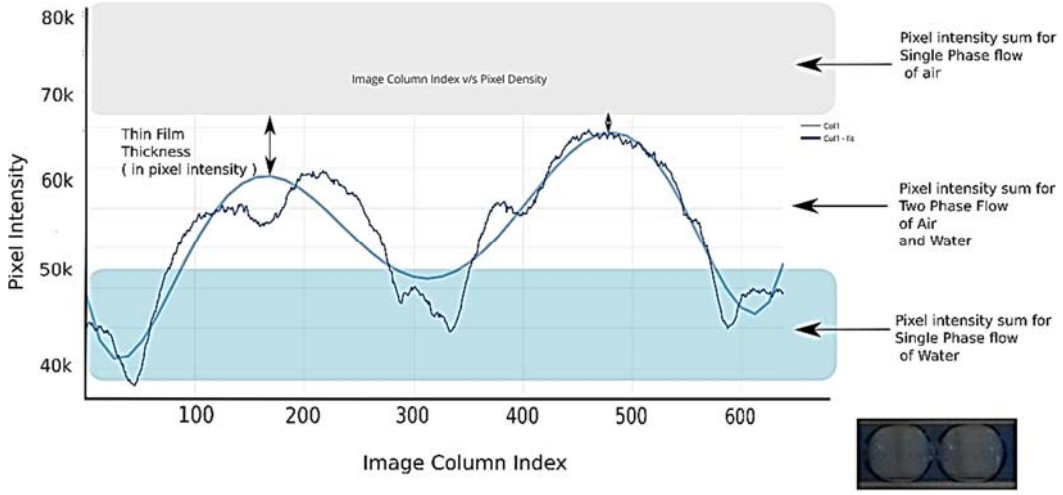

Fig. 10. Image Column Index v/s Pixel Intensity for Superficial liquid velocity 0.8 m/s and Superficial Gaseous Velocity 0.2 m/s. The obtained data and the data after a sixth degree polynomial curve fit are plotted.

The coefficients a1, a2 and a3 are found out by inversion of the matrix. With the values of coefficients known, the film thickness at any other point in the flow can be determined.

The following coefficient ranges were obtained in this study:

$a_1 \in (0.08, 0.195)$

$a_2 \in (0.1, 0.45)$

$a_3 \in (0, 0.1)$

From the above discussion, the thin film thickness for superficial liquid velocity of (0.4 - 1.5)m/s and superficial gaseous velocity of (0.2 - 0.4)m/s is obtained using Image Processing. (see Table 1 and 2).

A strong correlation between the two techniques is evident from the tabulation of the results.

It can be observed that there exists a positive error of a few millimetres in all the observed thin film thickness obtained using the optical method. This is due to the fact that the tube thickness was not taken into consideration for the model. Also, the error obtained does not exceed the tube thickness of 0.2 mm. This can easily accommodated by employing machine learning algorithms and devising an error function ε(t) that minimizes the positive error induced. Therefore, the optical method has unparalleled advantages over other methods mentioned in the literature and the image processing techniques. It is non-intrusive, fast and reliable which makes it stand out as a powerful method for the measurement of thin film thickness in laboratories and industries

6. CONCLUSION

Two Phase flow experiments were conducted on a glass tube of diameter 4.7 mm. Optical techniques were employed to determine the thin film thickness in two phase flows. The obtained values were validated using Image Processing.

It is concluded from the present study that the optical method yields accurate and reliable results for determining the thin film thickness. The optical method being easier in its set-up (involving no high-speed cameras for instance), experimental procedures and also faster processing time stands out as a powerful method for determination of thin film thickness in two phase flows. It remains as a future work to reduce the errors obtained through this method by employing a less divergent laser pointer and machine learning algorithms.

ACKNOWLEDGMENTS

The authors gratefully acknowledge the financial grant provided by DST/SERB Grant No. YSS/2015/000029 for carrying out this work.

REFERENCES

Balasubramanian, N., R. M. Anderson and W. H. Stevenson (1972). Feasibility of thin film thickness monitoring by holographic interferometry. *Journal of Vacuum Science and Technology 9*(3), 1080–1084.

Barrau, E., N. Rivire, C. Poupot and A. Cartellier (1999). Single and double optical probes in air-water two-phase flows: real time signal processing and sensor performance. *International Journal of Multiphase Flow 25*(2), 229–256.

Chen, X., T. Butler and J. P. Brill (1996). Capacitance probes for measurement of liquid film thickness *Proceedings of the ASME Heat Transfer Division at the International Mechanical Engineering Congress and Exposition 3*, 201208.

Coleman, J. W. and S. Garimella (1999). Characterization of two-phase flow patterns in small diameter round and rectangular tubes. *International Journal of Heat and Mass Transfer 42*(15), 2869–2881.

Dallman, J. C. (1978). *Investigation of separated flow model in annular gas-liquid two phase flows* Ph.D. thesis, University of Illinois at Urbana-Champaign, Urbana, IL.

Farias, P. S. C., F. J. W. A. Martins, L. E. B. Sampaio, R. Serfaty and L. F. A. Azevedo (2012). Liquid film characterization in horizontal, annular, two-phase, gas–liquid flow using time-resolved laser-induced fluorescence. *Experiments in Fluids 52*(3), 633–645.

Jagannathan, N., B. Chidambaram, A. Seshadri and V. Muniyandi (2015). Characterization of gas-liquid two-phase flows using laser patterns. *The Canadian Journal of Chemical Engineering 93*(9), 1678–1685.

Lai, Y. W., M. Krause, A. Savan, S. Thienhaus, N. Koukourakis, M. R. Hofmann and A. Ludwig (2011). High-throughput characterization of film thickness in thin film materials libraries by digital holographic microscopy. *Science and Technology of Advanced Materials 12*(5), 054201.

Lakehal, D. (2011). New trends in multiscale and multiphysics simulation of transport phenomena in novel engineering systems. *Journal of Advanced Fluid Mechanics 4*, 121–127.

Mouza, A. A., N. A. Vlachos, S. V. Paras and A. J. Karabelas (2000). Measurement of liquid film thickness using a laser light absorption method. *Experiments in Fluids 28*(4), 355–359.

Ruixi, D., Y. Da, W. Haihao, G. Jing, L. Ying, Z. Tong and Z. Lijun (2013). Optical method for flow patterns discrimination, slug and pig detection in horizontal gas liquid pipe. Flow *Measurement and Instrumentation 32*, 96 – 102.

Seshadri, A., S. Mahadevan and V. Muniyandi (2015). Measurement of liquid film thickness in air — water two phase flows in conventional and mini channels using image processing. *Korean Journal of Chemical Engineering 32*(5), 826–836.

Shedd, T. A. and T. A. Newell (1998). Automated optical liquid film thickness measurement method. *Review of Scientific Instruments 69*(12), 4205–4213.

Xue, T., L. Yang, P. Ge and L. Qu (2015). Error analysis and liquid film thickness measurement in gasliquid annular flow. Optik *International Journal for Light and Electron Optics 126*(20), 2674–2678.